Pressure-induced tricritical point in the ferroelectric phase transition of KH_2PO_4

Arthur B. Western,* Alan G. Baker,† Charles R. Bacon,‡ and V. Hugo Schmidt
Department of Physics, Montana State University, Bozeman, Montana 59717
(Received 20 December 1976; revised manuscript received 31 January 1978)

Measurement of the net polarization charge of two KH_2PO_4 crystals as a function of temperature, applied electric field, and hydrostatic pressure indicates the existence of a tricritical point in the (2.3 ± 0.3)-kbar pressure range. This result is based upon static measurements of the polarization response to applied dc field in a 0.5-K neighborhood of the ferroelectric transition at pressures of 0, 1, 2, 2.4, and 3 kbar. Unlike ^{3}He-^{4}He mixtures and some metamagnets, for KH_2PO_4 the field which gives rise to the "wing" structure of the tricritical point is experimentally available. For each of the five pressures the paraelectric region is well described by the Landau equation of state, $E = A_0(T-T_0)P + BP^3 + CP^5$, to within 0.05 K of the transition temperature. The exponent δ derived from our data at 3 kbar is in the crossover region between the critical value of 3 and the tricritical value of 5 predicted by Landau theory. At 2.4 kbar our derived value of δ is consistent with the tricritical value of 5. Analysis of the data along lines of constant polarization, which are here called "isopols," indicates that the transition is first order at 0 and 1 kbar with the critical field decreasing from 183 ± 60 V/cm at 0 kbar to 43 ± 13 V/cm at 1 kbar. At 3 kbar the B coefficient is positive which indicates a second-order transition. This observation of a change in the order of the transition is supported by a change in the behavior of the isothermal dielectric susceptibility which has a maximum for $E > 0$ at 0.5 kbar and at $E = 0$ at 3 kbar.

I. INTRODUCTION

A tricritical point was defined by Griffiths[1] as a point where three lines of critical points meet in a space of thermodynamic fields. For ^{3}He-^{4}He mixtures, the magnetic transition in $FeCl_2$, and the structural transition in NH_4Cl, one of the critical lines borders a first-order coexistence surface in a plane formed by two experimentally realizable fields. The other two critical lines border first-order surfaces which appear as symmetric "wings" to the first plane, but the ordering field necessary to examine the wing structure is not experimentally available. For example, in the antiferromagnetic case a staggered magnetic field with opposite direction on each sublattice would have to be applied.[2]

In the experimentally accessible zero-ordering-field plane the tricritical point is identified as the point where a first-order coexistence line (actually a line of triple points) changes to a second-order line. This latter possibility was discussed much earlier by Landau[3] who argued that a second-order coexistence line separating two phases of different symmetry can not end in a point. Rather, he proposed that a second-order phase boundary could terminate by changing continuously into a first-order line. Landau's phenomenological description is based upon the expansion of the free energy as a Taylor polynomial in the order parameter. In the case most often discussed the free energy has the form

$$F = \tfrac{1}{2}A_0(T-T_0)P^2 + \tfrac{1}{4}BP^4 + \tfrac{1}{6}CP^6 + \tfrac{1}{8}DP^8 + \cdots, \quad (1)$$

where T is the temperature and P is the order parameter. If terms of order P^6 and greater are positive definite then the order of the transition described by Eq. (1) depends upon the sign of B, being first order for $B < 0$ and second order for $B > 0$. If B changes smoothly from positive to negative as a function of some external parameter, then a "Landau tricritical point" is realized at $B = 0$.

The present work was motivated by the conjecture of Schmidt[4] that the ferroelectric crystal KH_2PO_4 (KDP) would exhibit a tricritical point with experimentally accessible wings in the space of temperature, electric field, and hydrostatic pressure. Since that time, Peercy[5] has shown that another ferroelectric, SbSI, has a tricritical point near 235 K and 1.40 kbar. In this paper we report on static measurements of the polarization of two KH_2PO_4 single crystals which indicate that such a tricritical point does exist. Thus far it has been possible to describe the crystal behavior in terms of the Landau phenomenological description of a tricritical point.

In Sec. II we review recent work by others concerning the order of KDP transition at ambient pressure and the effect of hydrostatic pressure on the transition temperature. Section III contains a description of our experimental configuration. Section IV is an introduction to the analysis of data along lines of constant polarization which we call "isopols." In Sec. V we present isopol data and results for the best fit coefficients in the Landau expression for free energy. Section VI compares measured critical exponents with predictions of

Landau theory. Section VII summarizes our findings and compares them with other recent results.

II. RECENT RELEVANT EXPERIMENTS

Prior to 1969 the ferroelectric transition in KDP at ambient pressure was generally thought to be second order.[6] Recent results indicate that it is in fact first order but quite close to being second order. This opinion is now supported by a number of experiments: Strukov *et al.*[7] exploited KDP's large electrocaloric effect and measured the temperature change produced by the sudden application of an electric field. Sidnenko and Gladkii[8] measured the polarization versus temperature of the crystal in various electric fields. Vallade[9] measured the temperature dependence of the polarization of KDP by optical birefringence. Okada and Sugié and others have studied the KDP transition extensively. They have reported on the temperature sweep rate dependence of the thermal hysteresis,[10] the difference between the adiabatic and isothermal dielectric constant,[11] and quasistatic measurements of the polarization versus applied field at constant temperature.[12] Reese and others have studied the transition in calorimetric[13] and electrocaloric[14] experiments. The most recent results of all of these groups are in fair agreement as to the coordinates of the critical point at the end of the first-order line (200–300 V/cm) and the fact that KDP obeys the phenomenological theory of Landau to within at least 0.1 K of the transition temperature.

There are, however, three experiments described in the literature which yielded markedly different results. The first of these is an x-ray dilatometric study by Kobayashi *et al.*[15] who found a critical field of 8500 V/cm, much higher than the critical fields of 200–300 V/cm found in the experiments described above. Matsuda and Abe[16] calculated the B coefficient in the Landau free energy from measurements of the third harmonic of a 1-kHz ac electric field applied to the crystal. Their value is two orders of magnitude larger (in absolute value) than reported in the papers cited earlier. Finally, Eberhard and Horn[17] studied the thermal hysteresis of the transition at various applied fields and concluded $E_{cr} = 6500$ V/cm. There is reason to believe[18] that this value should be revised downward closer to 300 V/cm.

The latest published results of all of these workers are displayed in Table I along with our previous results for two samples[19,20] and our presently reported results for a third sample. The parameters in Table I refer to the equation of state

$$E = A_0 (T - T_0) P + BP^3 + CP^5 + DP^7 \tag{2}$$

which follows from differentiating the free energy given in Eq. (1) with respect to P at constant temperature and pressure. Here E is the electric field, T is the temperature, and P is the polarization which acts as the order parameter for the transition. Values for the coordinates of the critical point at the termination of the first-order line have been calculated using

$$T_{cr} - T_0 = A_{cr}/A_0 = -(3BP_{cr}^2 + 5CP_{cr}^4 + 7DP_{cr}^6)/A_0 , \tag{3}$$

$$E_{cr} = A_{cr} P_{cr} + BP_{cr}^3 + CP_{cr}^5 + DP_{cr}^7 , \tag{4}$$

TABLE I. Recent published values of the parameters in the free energy $F = \frac{1}{2} A_0 (T - T_0) P^2 + \frac{1}{4} BP^4 + \frac{1}{6} CP^6 + \frac{1}{8} DP^8$ and derived coordinates of the critical point at ambient pressure.[a]

Reference	A (10^{-3} esu)	B (10^{-11} esu)	C (10^{-19} esu)	D (10^{-27} esu)	E_{cr} (V/cm)	$T_{cr} - T_0$ (K)
7	3.9	-1.9	6.3	0	120	0.07
8	3.8 ± 0.1	-3.0 ± 0.8	6.5 ± 1.1	0	370	0.16
	3.8 ± 0.1	-0.5 ± 0.3	0	3.8 ± 0.4	87	0.036
9	3.9	-0.54 ± 0.05	0	2.85 ± 0.10	124	0.046
	3.9	-1.85 ± 0.25	3.3 ± 0.5	0.87 ± 0.5	280	0.11
12	4.2 ± 0.1	-1.9 ± 0.1	5.4 ± 0.4	0	160	0.07
14	(3.81)	-0.44	0	2.96	84	0.055
15	(3.86)	-11.9	11.0	0	8500	1.50
16	...	-110	...	...	...	...
17	(7.3)[b]	-2.2	0.6	0	6500	0.51
Our work						
19 (Sample 1)	4.3 ± 0.2	-2.35 ± 0.4	5.91 ± 1.5	0	232 ± 70	0.10 ± 0.03
20 (Sample 2)	4.0 ± 0.2	-1.48 ± 0.2	3.1 ± 0.4	0	186 ± 60	0.08 ± 0.03
(Sample 3)	3.91 ± 0.04	-1.26 ± 0.05	3.2 ± 0.1	0	123 ± 18	0.057 ± 0.007

[a] Numbers in parentheses were obtained from a source other than the primary reference.
[b] Reference 18.

where P_{cr} is given by

$$P_{cr}^2 = (5C/21D)[(1 - 63BD/25C^2)^{1/2} - 1], \quad C \neq 0, \ D \neq 0,$$
$$P_{cr}^2 = (-B/7D)^{1/2}, \ C = 0, \ D \neq 0, \tag{5}$$
$$P_{cr}^2 = -3B/10C, \ C \neq 0, \ D = 0.$$

There has been considerable discussion[7,12,14] concerning the proper form for the saturation function of the free energy, i.e., which of the terms of order greater than P^3 should be included in Eq. (2) in order to give the "best" description of the large polarization response of KDP. At present a quantitative comparison of the results of various authors is not possible. It would be particularly useful if the method of orthogonal polynomials[21] were applied to such polarization data so that statistically quantitative statements could be made regarding the degree of fit of various forms for the saturation function. In our experiment the reduction of the residual sum of squares resulting from the addition of a DP^7 term was not statistically significant. This was expected as polarization values obtained in the paraelectric region were not large enough to resolve higher-order terms.

The effect of hydrostatic pressure on the transition temperature of KDP has been studied using neutron scattering by Umebayashi *et al.*[22] and in dielectric experiments by Hegenbarth and Ullwer[23] and by Samara.[24] In these experiments the temperature resolution was not sufficient to differentiate between the Curie-Weiss temperature T_0 and the actual transition temperature T_c, so we compare the above measurements of dT_c/dp with our findings for dT_0/dp in Table II. The value of $dT_0/dp = 4.54 \pm 0.05$ K/kbar obtained in this work is in agreement with those of Umebayashi *et al.*[22] and Samara.[24]

III. EXPERIMENTAL

The preparation of the first crystal and results obtained from it at ambient pressure have been described previously.[19] The second KDP single crystal was obtained from Cleveland Crystals, Inc.[25] and stored in a vial with $CaSO_4$ desiccant for 20 months. Crystal dimensions were $1 \times 1 \times 0.2$ cm^3, the large faces being perpendicular to the ferroelectric c axis. Chrome-gold electrodes had been evaporated onto the surface by the supplier. The 0.0025-in. diameter Solid Copperweld center wires (copperplated steel wires) of Type *A* Ultraminiature Coaxial Cable[26] were attached to the evaporated electrode faces by means of silver paint[27] applied as small (~4 mm^2) dots on either side. Five coats were used in an effort to increase the strength of the bond as these lead wires were the sole support for the crystal. Thus the only stress on the unpressurized freely hanging crystal was that caused by its own weight.

TABLE II. Summary of reports of the effect of pressure on the ferroelectric transition temperature of KH_2PO_4.

Reference	dT_0/dp, (K/kbar)	Method
22	-4.52 ± 0.06	Neutron scattering
23	-5.6	Dielectric constant
24	-4.6 ± 0.1	Dielectric constant
Present work	-4.54 ± 0.05	Isopols

A corner of the second crystal broke off during apparatus disassembly after the end of the 3-kbar run. The remaining work was carried out with a third crystal of the same dimensions and suspended in the same way as the second crystal. This crystal was obtained from Cleveland Crystals, Inc.[25] about two months before it began service as a sample.

In order to check crystal quality the small signal (0.05 V/cm) ac dielectric constant ϵ was measured at 1 kHz. From $T_c + 0.3$ K to T_c a straight line was obtained for ϵ^{-1} vs T in accordance with the Curie-Weiss law. The second crystal showed a slight decrease in ϵ at 40 mK above T_0, then the dielectric constant rose to 360 000 after which it stayed constant for at least 0.2 K below T_0. The third crystal had a peak dielectric constant of 430 000.

Conventional wisdom attributes the above behavior to domain wall motion. Bornarel, Fousková, Guyon, and Lajzerowicz[28] showed that the dielectric constant 12 K below T_c could be reduced from 4.5×10^4 to 1.4×10^4 by reducing the size of the applied ac fields from 2 V/cm to 0.5 V/cm. This would seem to support the domain wall explanation. In the course of this investigation ac fields as small as 0.005 V/cm were used in a 0.3 K neighborhood of T_c with slight reduction in dielectric constant, but no change in the temperature dependence. If domain wall motion is responsible for the high dielectric constant in the ferroelectric region, the walls are very mobile indeed immediately below T_c.

The sample was suspended in a beryllium-copper[29] pressure vessel (PV) surrounded by two concentric cylindrical cans with 0.25-in. diameter high-pressure tubing acting as the central connecting axis. A schematic drawing of the cryostat is shown in Fig. 1. The region of the cryostat external to the PV was evacuated to 10^{-4} Torr or better and the entire assembly immersed in a dewar of liquid nitrogen. The point where the pressure tubing passes through the inner copper shield can, marked *C* in Fig. 1, was held at a fixed (± 0.1 K)

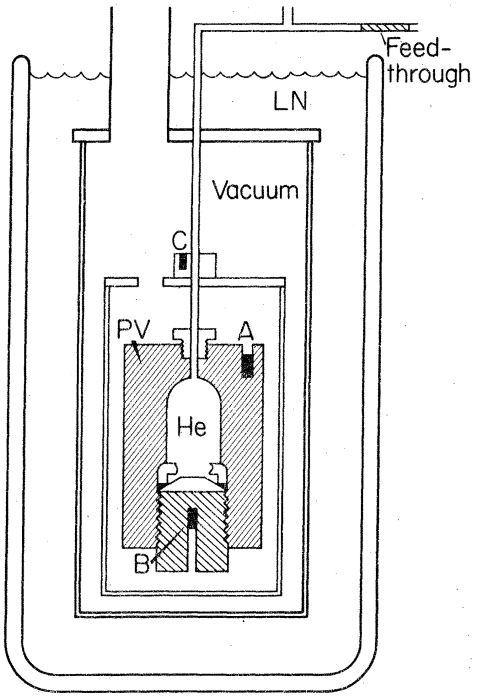

FIG. 1. Schematic drawing of cryostat used to control pressure vessel (PV) temperature. A copper-constantan thermocouple was located at C, and capacitance thermometers at A and B.

temperature about 3 K below the PV temperature by means of heater current controlled by a feedback amplifier using a copper-constantan thermocouple located at point C as the temperature sensor.

The temperature of the PV itself was regulated using a commercial temperature controller[30] employing as the temperature sensor a glass-encapsulated capacitor with strontium titanate dielectric,[31] located at point A of Fig. 1. The temperature of the sample was assumed to be the same as that of a second capacitor embedded in the closure plug of the PV, point B in Fig. 1. Care was taken to maintain a constant temperature difference between the two sensors over the temperature intervals studied. The temperature sensors were calibrated *in situ* against copper-constantan thermocouples using a Leeds and Northrup K-5 Potentiometer and distilled water ice bath. In the temperature range studied the controller has a temperature resolution of ± 2 mK and the pressure-vessel temperature can be held stable with this precision for arbitrary lengths of time.

The sample was pressurized with helium gas using a diaphragm pump and intensifier. The pressure was determined using a Cary-Foster[32]-type Wheatstone bridge to measure the resistance of a thermostated manganin cell. The resistance was measured with an accuracy equivalent to ± 50 psi and the stability monitored with a precision of ± 1 psi. As Table II shows, the crystal transition temperature changes as a function of pressure. In order to maintain the crystal transition temperature constant to ± 2 mK the pressure was maintained constant to within ± 0.5 bar by occasional pumping to offset a leak from the manganin cell.[33] Such pumping disturbed the equilibrium of the crystal and care was taken to allow the crystal to return to the steady state before resuming measurements. Modeling the pressure-system leaks as an isentropic throttling process indicates that at the maximum pressure leak rate (~ 1 bar/h at 3 kbar) the flow work proceeded at a rate of ~ 1 mW. Since this amount of power is easily exchanged between the pressurized helium gas and the pressure tubing, the finite pressure leak had negligible cooling effect on the crystal. The electrical stability of the pressure-measuring system was monitored at a known pressure of 1 bar and found to be equivalent to ± 0.7 bar over a period of three days.

Static electric fields were applied to the crystal using a battery and resistive voltage divider. Polarization charge was stored on an 8-μF polystyrene capacitor in series with the sample. The resultant voltage was measured with a high-impedance (10^{12} Ω) electrometer.[34] The measurement circuit had an RC time constant of 8×10^6 sec, resulting in a maximum leak rate of 1.1%/day. Stray charge leakage was maintained below this value by the use of Teflon insulation and careful guarding. Further experimental details may be found elsewhere.[35]

IV. ISOPOLS

There is a tradition in the literature of measuring polarization (P) as a function of electric field (E) along isotherms, or as a function of temperature (T) along isochamps. Most of the data to be presented here is displayed as a function of T and E along lines of constant polarization, i.e., along isopols. This approach appears to be new and thus the following discussion is devoted to the interpretation of such plots. This discussion is based upon the Landau equation of state given in Eq. (2); however, many of the conclusions based on isopol plots are independent of this equation of state. The reader is cautioned not to equate the validity of all conclusions with the validity of the Landau expansion which is used here merely as a vehicle for introducing the isopol picture.

The equation of state [Eq. (2)] which follows from the Landau free energy given in Eq. (1), when

rewritten, indicates that the isopols are straight lines in the T-E plane with slopes $(A_0P)^{-1}$ and $E=0$ intercepts $T_0-(BP^2+CP^4)/A_0$; i.e.,

$$T=(A_0P)^{-1}E+T_0-(BP^2+CP^4)/A_0. \quad (6)$$

In the limit of small P the $E=0$ intercepts tend to T_0. If B is negative, when P increases the intercepts rise above T_0 and then fall as P increases further and the CP^4 term begins to dominate. For B positive the intercepts simply fall farther and farther below T_0 as P increases. The case for negative B is shown in Fig. 2.

The initial increase and subsequent decrease in the T intercepts creates a region where isopols intersect. The first-order line, FD in Fig. 2, lies within the overlap region which is bounded by caustics $ACDB$. Note that BCE is the extension of a line similar to BD in the negative E half plane not shown in Fig. 2. The critical point D is at a vertex of the curvilinear triangle formed by the caustics of intersecting isopols. Isopols are shown as solid lines when they correspond to an absolute minimum of the free energy. After crossing the first-order line they are shown as dashed lines and correspond to local minima of the Landau free energy.

If metastable states corresponding to local minima are actually manifested by the crystal, mixed

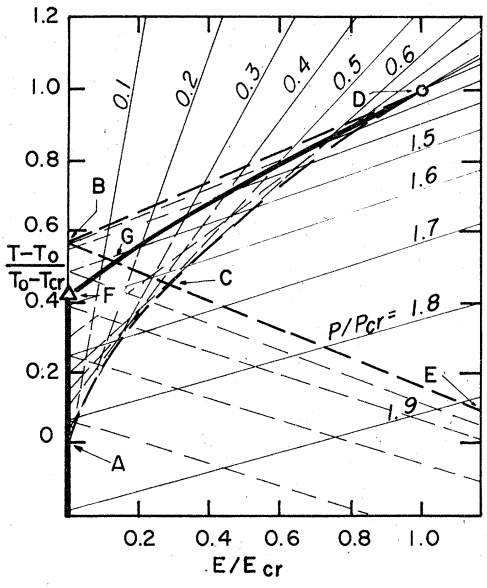

FIG. 2. Phase diagram for a first-order transition as described by $E=A_0(T-T_0)P+BP^3+CP^5$. Triangle is Curie point or triple point. Circle is the critical point. Heavy solid lines indicate first-order transitions. Light solid and dashed lines correspond to isopols for stable and metastable phases, respectively. Heavy dashed lines outline limits of regions of metastability.

TABLE III. Possible mixed phase regions in Fig. 2. Phases corresponding to absolutely stable minima of the free energy are denoted S, states corresponding to relative minima are denoted M. The polarization is "up" when parallel to the applied E field.

Region	Paraelectric	Ferroelectric "up"	Ferroelectric "down"
BDG	S	M	
CDG	M	S	
BGF	S	M	M
$AFGC$	M	S	M
ACE		S	M

phases exist in the regions of isopol overlap. Denoting regions of polarization parallel to $+E$ as "up," the mixed phase regions may be characterized as in Table III. We have shown elsewhere[19] that when an experimental isopol crosses a line such as CE in Fig. 2, it changes direction, heading almost vertically downward. This is interpreted as resulting from the creation of mixed phases in the form of ferroelectric domains within the crystal.

In the Landau equation of state the order of the transition is indicated by the sign of the coefficient B, being negative for first order and positive for second order. In an isopol plot this difference manifests itself as a convergence or nonconvergence of isopols, respectively. The deduction of the order of the transition from the behavior of isopols is, however, independent of the Landau equation of state. This may be seen by considering an isotherm drawn through an isopol plot just above T_{cr} (see Fig. 2). If the isopols converge toward an $E\neq0$ point, then the isotherm will encounter a large change in polarization for a small change in field near the point of convergence, i.e., the dielectric susceptibility will be high. A dielectric susceptibility higher at $E>0$ than at $E=0$ indicates an $E\neq0$ critical point, and thus a first-order transition at $E=0$ is implied. On the other hand, if the isopols do not converge except for $E=0$ then the dielectric susceptibility is never higher than at $E=0$, and a second-order transition at $E=0$ is indicated.

The advantage of displaying data in isopol plots rather than as electric field dependence of the dielectric susceptibility is the numerical convenience and graphical clarity afforded by fitting straight lines. In addition, deviation from the simple Landau picture becomes obvious when the actual crystal isopols deviate from the high-temperature extrapolations.

Two methods were used for extracting Landau parameters from isopol data. The first method

begins with calculation of a least-squares straight-line fit to paraelectric isopols. From these, A_0 is obtained from the slopes of the isopols using

$$A_0 = (\partial E/\partial T)_P/P. \tag{7}$$

An approximate value of T_0 is found from a plot of the extrapolated $T(E=0)$ intercepts versus P^2 for the three smallest isopols. This plot is a straight line and should extrapolate to T_0. The parameters B and C are then deduced from the intercept and slope respectively of a graph of $-A_0(T-T_0)/P^2$ vs P^2. In practice T_0 is then varied a small amount (within the experimental error) to produce the best straight line on this graph. In this latter procedure, points from the higher-polarization isopols are heavily weighted owing to the large scatter produced on this type of graph by the low-polarization isopols for which $T-T_0$ is quite small.

The second method begins with calculation of the average temperature $\langle T_i\rangle$ and average field $\langle E_i\rangle$ for the data points for each isopol. The A_{0i} for the various isopols are then calculated as described above, and their weighted average A_0 is obtained. The Landau equation of state predicts that

$$\langle T_i\rangle = T_0 + \langle E_i\rangle/A_0P_i - P_i^2B/A_0 - P_i^4C/A_0 \tag{8}$$

for the isopol corresponding to polarization P_i. These equations for the various isopols are solved simultaneously for the values of T_0, B, and C which give the best fit to the measured $\langle T_i\rangle$, taking the differences in the standard deviations of the $\langle T_i\rangle$ into account with appropriate weighting factors. Mathematical details of this method appear elsewhere.[36]

The first calculational method was used for the first two crystals, and the second method for the third crystal. Both methods were used for the 3-kbar data for the second crystal and the ambient-pressure data for the third crystal, and the results agreed within experimental error.

V. EXPERIMENTAL RESULTS

Isopol data for sample 2 at pressures of 0, 1, and 3 kbar are presented in Figs. 3–5. Each data point was taken as close to equilibrium as possible. Finite pressure leaks necessarily led to finite polarization drift. The largest leak rate was 1 bar/h at 3 kbar which is equivalent (see Table II) to a temperature drift of 5 mK/h. At "equilibrium" the polarization drift rate was less than 2%/h in all cases. Tables IV–VI summarize the best fit Landau parameters. The data can be fit satisfactorily with these Landau parameters at

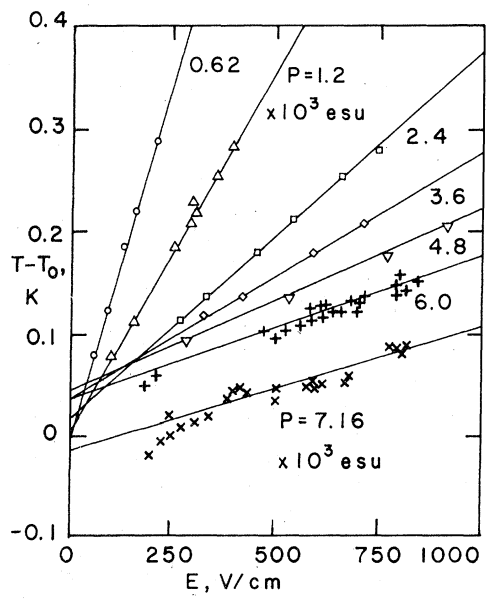

FIG. 3. Isopols at 0 kbar. Solid lines are generated from Landau equation of state, $E = A_0(T-T_0)P + BP^3 + CP^5$, for best-fit parameters. Intersection of extrapolated isopols indicates a first-order transition.

all three pressures. Crossing of extrapolated isopols in Fig. 3 indicates the first-order nature of the transition graphically. Based upon the best-fit Landau parameters, the ambient-pressure critical field of 186 ± 60 V/cm is reduced to 44 ± 13 V/cm by 1 kbar of hydrostatic pressure. At 3

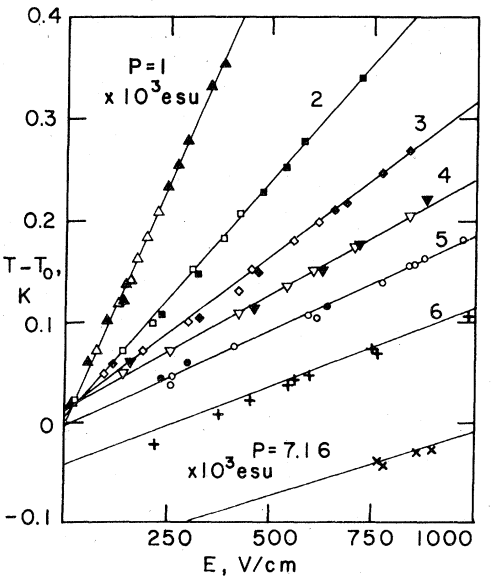

FIG. 4. Isopols at 1 kbar. Solid lines are generated from Landau equation of state, $E = A_0(T-T_0)P + BP^3 + CP^5$, for best-fit parameters. Intersection of extrapolated isopols indicates a first-order transition.

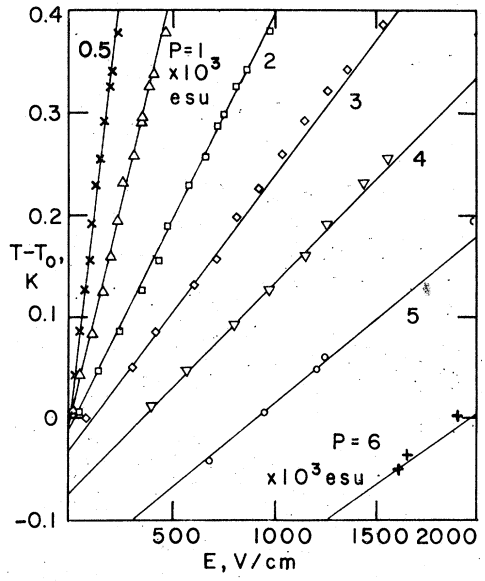

FIG. 5. Isopols at 3 kbar. Solid lines are generated from Landau equation of state, $E + A_0(T - T_0)P + BP^3 + CP^5$, for best-fit parameters. Extrapolated isopols do not cross, which indicates a second-order transition.

kbar the transition appears to be second order, that is, the extrapolated intercepts all fall below T_0.

This conclusion regarding the change of the order of the transition is supported by a change in the behavior of the isothermal dielectric constant as deduced from the slope of P vs E traces taken for sample 2 at constant temperature and pressure, and at electric field sweep rates of 240 V/cm h. At 0.5 kbar the maximum dielectric constant occurred at 300 V/cm while at 3 kbar the dielectric constant was highest at $E = 0$. Landau parameters and critical fields deduced from such plots are in general agreement with those extracted from isopol data, but the values appear to depend upon the electric field sweep rate. Nonetheless, we consider the difference in shape, as shown in Fig. 6, to be highly significant. (See Ref. 12 for details concerning this technique.)

Additional isopol data were obtained with sample 3 at pressures of 0, 2, and 2.4 kbar. Graphs of these isopols are not shown here, but the fit to the Landau parameters is as good as for the sample 2 data shown in Figs. 3–5. The best fit Landau parameters for the sample 3 isopols are given in Tables VII–IX. Table IX shows an apparently systematic decrease in A_0 from run to run for the three runs having total duration of six weeks. Such systematic decrease could be caused by increase of effective contact area, but there was no visual evidence of defective contacts after the runs, so the origin of this systematic variation is unknown. The best fit Landau parameters A_0, B, and C reported previously[19,20] for samples 1 and 2 and reported now[37] for sample 3 are presented in Table X. The B and C values are not dependent upon the values assigned to A_0, and were determined by the methods described in Sec. IV. The results for B as a function of pressure p are shown in Fig. 7 for all three samples. A least-squares linear fit[38] to all seven points yields $B = 0$ at 2.18 kbar, while linear fits to the sample 2 and sample 3 points give 1.94 and 3.02 kbar, respectively. If a quadratic term is included, the corresponding pressures are 2.36, 2.11, and 2.42 kbar. Based on these results we consider the tricritical pressure to be 2.3 ± 0.3 kbar.

VI. CRITICAL EXPONENTS

From the isopol plots in Figs. 3–5 we have seen that KH_2PO_4 obeys Landau theory in the regions of

TABLE IV. Data for Sample No. 2 at 0.0016 kbar. Here and in Tables V – IX, $\Delta = [(A_0 - \bar{A}_0)^2/(n-1)]^{\frac{1}{2}}$, where n is the number of values of A_0. Confidence intervals are tabulated here and in Tables V and VI because the standard errors do not accurately indicate the uncertainties in the A_0 values for the small N values in these tables.

P (10^3 esu)	N	A_0 (10^{-3} esu)	Standard error (10^{-3} esu)	95% confidence interval	$T - T_0$ (mK)	Standard error (mK)	95% confidence interval
0.621	7	3.91	0.05	0.13	9.8	3.0	7.7
1.194	8	3.90	0.047	0.12	4.9	2.8	6.9
2.388	6	4.07	0.06	0.17	27.2	2.8	7.8
3.582	5	4.21	0.029	0.09	47.3	0.9	2.7
4.776	4	3.95	0.071	0.31	41.9	7.7	22.8
5.97	16	3.52	0.144	0.31	21.0	4.3	9.1
7.167	9	4.09	0.375	0.89	-12.5	6.7	15.8
		$\bar{A}_0 = 4.01$	$\Delta = 0.13$	0.19			

TABLE V. Data for sample No. 2 at 1.00 kbar.

P (10^3 esu)	N	A_0 (10^{-3} esu)	Standard error (10^{-3} esu)	95% confidence interval	$T - T_0$ (mK)	Standard error (mK)	95% confidence interval
Decreasing temperature							
1.00	12	3.62	0.062	0.14	2.7	4.2	9.4
2.00	10	3.61	0.081	0.19	7.6	5.5	12.7
3.00	6	3.81	0.15	0.42	21.4	6.7	18.6
4.00	4	3.80	0.14	0.60	23.2	4.5	19.4
Increasing temperature							
1.00	8	3.62	0.084	0.21	3.1	3.6	8.8
2.00	6	3.56	0.114	0.32	7.6	4.5	12.5
3.00	6	3.74	0.12	0.33	20.5	4.5	12.5
4.00	6	3.60	0.05	0.14	15.6	2.0	5.6
5.00	9	3.52	0.064	0.15	- 2.7	2.2	5.2
6.00	8	3.56	0.165	0.16	-43.7	1.8	4.3
7.167	Not calculated			assuming $\bar{A}_0$	-147.5	NA	NA
		$\bar{A}_0$ = 3.64	Δ = 0.11	0.08			

p-T-E space in which we made measurements. To determine which of our data points fall in the critical region and which in the tricritical region we examine the behavior of the critical exponents which can be derived from our data.

The exponents β, γ, and δ are associated with dielectric properties. However, we cannot determine β from our macroscopic dielectric measurements because it depends on the value of P in the stable phase near first-order transition surfaces in p-T-E space, and near such surfaces our results correspond to an average of P over the crystal, part of which is in the stable phase and part in metastable phases, as discussed in Sec. IV.

We now examine predictions of Landau theory for the critical exponents γ and δ based on expansion of the free energy F in terms of the order parameter, $P - P_{cr}$. We truncate F in Eq. (1) after the P^6 term. To locate the critical lines we evaluate the derivatives

$$\begin{aligned} &\partial F/\partial P = E = P(A + BP^2 + CP^4), \\ &\partial^2 F/\partial P^2 = (\chi_T)^{-1} = A + 3BP^2 + 5CP^4, \\ &\partial^3 F/\partial P^3 = 2P(3B + 10CP^2), \\ &\partial^4 F/\partial P^4 = 6(B + 10CP^2), \end{aligned} \tag{9}$$

and note that the conditions that the susceptibility be infinite at critical points and positive everywhere require that at critical points $\partial^2 F/\partial P^2 = \partial^3 F/\partial P^3 = 0$ and $\partial^4 F/\partial P^4 \geq 0$. These conditions give a central critical point at $E_{cr} = P_{cr} = A_{cr} = 0$ if $B > 0$, and give wing critical points at $E_{cr} = 8CP_{cr}^5/3$, $P_{cr} = \pm(-3B/10C)^{1/2}$, $A_{cr} = 9B^2/20C$ if $B < 0$. Both the central and wing critical points found by this procedure are stable according to the bitangent con-

TABLE VI. Data for sample No. 2 at 3.00 kbar.

P (10^3 esu)	N	A_0 (10^{-3} esu)	Standard error (10^{-3} esu)	95% confidence interval	$T - T_0$ (mK)	Standard error (mK)	95% confidence interval
0.50	14	4.23	0.085	0.19	+10.6	5.8	12.6
1.00	15	4.13	0.071	0.15	- 2.4	4.8	10.4
2.00	16	4.09	0.054	0.12	-15.8	3.8	8.1
3.00	16	4.10	0.054	0.12	-30.0	4.0	8.6
4.00	9	3.90	0.085	0.20	-82.4	5.2	12.3
5.00	5	3.74	0.039	0.12	-169	2.4	7.0
6.00	3	3.53	0.106	1.35	-309	8.0	101.0
		$\bar{A}_0$ = 4.04	Δ = 0.18	0.20			

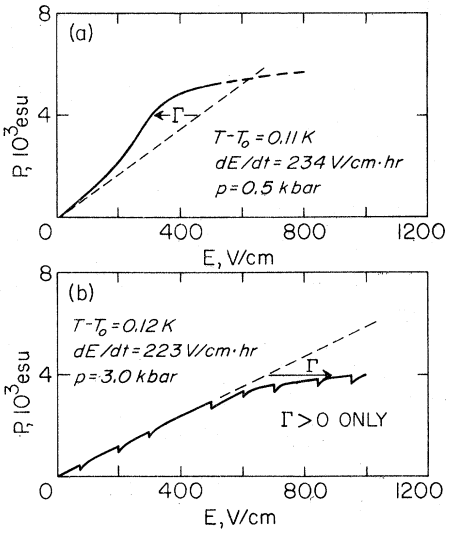

FIG. 6. Polarization vs electric field at constant temperature, at an electric field sweep rate of ~230 V cm^{-1} h^{-1}. At 0.5 kbar (a) the maximum dielectric constant occurs at ~300 V cm^{-1}, while at 3 kbar (b) the dielectric constant is a maximum at $E=0$. Spikes in 3-kbar trace are due to pressure pumps. Here $\Gamma = E - A_0(T-T_0)P = BP^3 + CP^5$.

struction criterion.[39] Because A and B depend on temperature T and pressure p, three lines consisting of central and wing critical points can be constructed in p-T-E space, and these lines meet at the tricritical point, which is characterized by $E_t = P_t = A_t = B_t = 0$.

A Taylor expansion of the free energy about a critical point using Eqs. (9) yields

$$\begin{aligned} F = F_{cr} &+ [(A-A_{cr})P_{cr} + E_{cr}](P-P_{cr}) \\ &+ \tfrac{1}{2}(A-A_{cr})(P-P_{cr})^2 \\ &+ \tfrac{1}{4}(B+10CP_{cr}^2)(P-P_{cr})^4 \\ &+ CP_{cr}(P-P_{cr})^5 + \tfrac{1}{6}C(P-P_{cr})^6. \end{aligned} \quad (10)$$

We now examine predictions for the exponents γ and δ based on this expansion.

The exponent γ is defined by

$$\chi_T = (\partial^2 F/\partial P^2)^{-1} = (A + 3BP^2 + 5CP^4)^{-1} \propto \epsilon^{-\gamma}, \quad (11)$$

where $\epsilon = (T - T_{cr})/T_{cr}$. For the central critical line, χ_T is evaluated for $E = P = 0$, $A > 0$. Since $A = A_0(T - T_0)$ in lowest order, and $T_0 = T_{cr}$ for this critical line, the exponent $\gamma = 1$ is obtained. To arrive at an analogous definition of γ for the wing critical lines, χ_T must be evaluated for $P = P_{cr}$, $A > A_{cr}$, and again $\gamma = 1$ is obtained. [Note that the requirement $P = P_{cr}$ used in evaluating $E = \partial F/\partial(P - P_{cr})$ from Eq. (9) yields $E = E_{cr} + (A - A_{cr})P_{cr}$, so that E and T must be varied simultaneously in finding the temperature dependence of the susceptibility as needed to evaluate γ.] At the tricritical point the relation $\gamma = 1$ is still obtained, so that a distinction between critical and tricritical regions cannot be made on the basis of γ.

The exponent δ is defined by $E = \partial F/\partial P \propto P^\delta$. For the central critical line, E is evaluated for $T = T_{cr}$ ($A = A_{cr} = 0$), so that $E = BP^3 + CP^5$, yielding $\delta = 3$. A corresponding definition of δ for the wing critical lines requires that E be evaluated for $A = A_{cr}$, yielding

$$\begin{aligned} E - E_{cr} = &-2B(P-P_{cr})^3 \pm (-15BC/2)^{1/2}(P-P_{cr})^4 \\ &+ C(P-P_{cr})^5 \end{aligned} \quad (12)$$

as obtained by substituting $P_{cr} = \pm(-3B/10C)^{1/2}$ into $E = \partial F/\partial(P - P_{cr})$, using Eq. (10) for F. Again, $\delta = 3$ is obtained, but the lack of symmetry near the wing critical points is reflected by the $(P - P_{cr})^4$ term whose sign depends on whether E is above or below E_{cr}. At the tricritical point we have $B = 0$, so $E = CP^5$ and $\delta = 5$. If crossover from $\delta = 3$ to $\delta = 5$ is defined to occur where the $C(P - P_{cr})^5$ term is as large as the other terms(s), then crossover occurs for $(P - P_{cr}) \propto B^{1/2}$ or, equivalently, for

TABLE VII. Data for sample No. 3 at 0.001 kbar.

P (10^3 esu)	N	A_0 (10^{-3} esu)	Standard error (10^{-3} esu)	$T(E=0) - T_0$ (mK)	Standard error (mK)
0.50	39	3.91	0.05	1.6	0.9
1.00	41	3.91	0.05	3.6	0.8
2.00	39	3.87	0.05	10.5	0.8
3.00	34	3.92	0.07	26.4	0.9
4.00	25	3.92	0.10	32.5	1.0
5.00	22	4.10	0.16	34.1	1.2
6.00	28	4.10	0.16	10.0	0.9
7.00	10	3.70	0.43	-38.0	2.9

$\bar{A}_0 = 3.93 \quad \Delta = 0.13$

TABLE VIII. Data for sample No. 3 at 2.00 kbar. The data have been adjusted to compensate for an apparent rise in T_0 of 4.7 mK/day during this 20-day run.

P (10^3 esu)	N	A_0 (10^{-3} esu)	Standard error (10^{-3} esu)	$T(E=0)-T_0$ (mK)	Standard error (mK)
0.50	24	3.97	0.08	-1.5	3.7
1.00	23	4.05	0.07	4.5	3.3
2.00	23	3.98	0.08	2.6	3.7
3.00	22	4.04	0.07	2.8	3.2
4.00	20	4.02	0.10	-12.2	4.4
5.00	14	3.63	0.08	-57.6	3.3
6.00	9	3.62	0.20	-122.0	7.9
7.00	5	2.57	0.88	-290.1	72.1
		$\bar{A}_0 = 3.90$	$\Delta = 0.19$ (omitting 7000 esu value)		

$(E-E_{cr}) \propto B^{5/2}$, evaluated on the $A = A_{cr}$ surface on which δ is defined. Because $B \propto (p-p_t)$ in lowest order, these crossover exponents occur also in the relations

$$|P-P_{cr}| \propto |p-p_t|^{1/2}, \quad |E-E_{cr}| \propto |p-p_t|^{5/2}, \tag{13}$$

both above and below the tricritical pressure p_t.

We now present comparisons of these predictions for γ and δ with our experimental results. We approximated $\chi_T = (\partial P/\partial E)_{P=0,T}$, which appears in the definition of γ, by P/E for the lowest P (500 esu) isopol for the 3-kbar data, because for this pressure the isopol extends all the way to $E=0$,

TABLE IX. Data for sample No. 3 at 2.40 kbar.

P (10^3 esu)	N	A_0 (10^{-3} esu)	Standard error (10^{-3} esu)	$T(E=0)-T_0$ (mK)	Standard error (mK)
Decreasing temperature					
0.50	9	3.84	0.06	-9.9	1.4
1.00	8	3.92	0.04	-2.5	1.1
2.00	10	4.00	0.06	-0.7	1.3
3.00	10	3.94	0.06	-8.6	1.3
4.00	6	4.15	0.05	-18.7	1.1
5.00	5	3.94	0.14	-60.2	1.8
		$\bar{A}_0 = 3.97$	$\Delta = 0.10$		
Increasing temperature					
0.50	6	3.87	0.09	0.0	1.5
1.00	6	3.81	0.19	-0.7	3.1
2.00	6	3.87	0.06	-0.2	1.2
3.00	6	3.85	0.19	-4.0	2.1
4.00	4	3.70	0.07	-29.3	1.1
5.00	2	3.44	...	-77.3	...
		$\bar{A}_0 = 3.76$	$\Delta = 0.17$		
Decreasing temperature					
0.50	16	3.51	0.29	-1.1	4.3
1.00	17	3.41	0.26	-3.8	4.1
2.00	18	3.52	0.24	+2.5	3.6
3.00	21	3.36	0.20	-13.0	3.2
4.00	20	3.36	0.16	-28.1	2.7
5.00	16	3.01	0.16	-79.0	2.9
6.00	8	2.78	0.25	-155.6	4.3
		$\bar{A}_0 = 3.28$	$\Delta = 0.28$		
		$\bar{A}_0 = 3.85 \pm 0.09$ (weighted average of the averages for the 3 runs)			

TABLE X. Landau coefficients for three KH_2PO_4 crystals at various hydrostatic pressures. The A_0 values listed below are averages weighted by the inverse squares of the standard errors for individual isopols given in Tables IV - IX, and accordingly differ somewhat from the unweighted $\bar{A}_0$ averages listed in those Tables.

P (kbar)	Sample No.	A_0 (10^{-3} esu)	B (10^{-11} esu)	C (10^{-19} esu)
0.001	1	4.3 ± 0.2	-2.35 ± 0.40	5.9 ± 1.5
0.0016	2	3.93 ± 0.07	-1.48 ± 0.05	3.1 ± 0.2
0.001	3	3.91 ± 0.03	-1.26 ± 0.05	3.18 ± 0.13
1.00	2	3.64 ± 0.08	-0.89 ± 0.05	3.6 ± 0.2
2.00	3	3.90 ± 0.19	-0.64 ± 0.06	5.88 ± 0.14
2.40	3 (run 1)	3.98 ± 0.03	-0.02 ± 0.08	4.2 ± 0.3
2.40	3 (run 2)	3.80 ± 0.05	-0.31 ± 0.36	8.9 ± 1.7
2.40	3 (run 3)	3.30 ± 0.08	+0.03 ± 0.24	4.4 ± 0.6
2.40	3 (wtd. av.)	3.89 ± 0.03	-0.03 ± 0.07	4.4 ± 0.3
3.00	2	4.04 ± 0.10	+0.90 ± 0.05	6.1 ± 0.2

$T = T_0$. All of the points on this isopol, as shown in Fig. 5, were used to determine γ in the relation $\chi_T \propto [(T - T_0)/T_0]^{-\gamma}$. With T_0 set at the value obtained from a best fit to all of the isopols, the value $\gamma = 1.03 \pm 0.04$ resulted. With T_0 and γ both allowed to vary to give the best fit to the 500-esu isopol, the value $\gamma = 1.01 \pm 0.02$ was obtained. Accordingly, the value of γ obtained from that data most suited for its determination shows no significant deviation from the mean-field value of 1.

To determine δ, we analyzed $E(P, T = T_{cr})$ for the data from samples 2 and 3. Because the experimental points show no systematic deviation from straight lines, we determined E from the equation of state:

$$E = A_0(T - T_0)P + BP^3 + CP^5, \tag{14}$$

in which A_0 and $T - T_0$ are best fit values for the slope and intercept of each individual isopol as given in Tables IV–IX. The uncertainties for these E values were calculated from the uncertainties for A_0 and $T - T_0$ given in those tables.

The results of this analysis for $p = 3$ kbar are shown in Fig. 8. The reliable data points all fall in the crossover region. Similar plots (not shown) for the 0 and 1 kbar results consist of points which

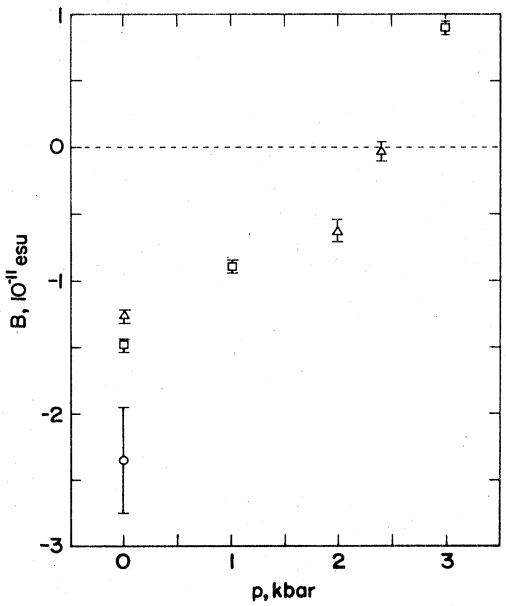

FIG. 7. Plot of Landau B coefficient vs pressure p for KH_2PO_4 sample 1 (circle), sample 2 (squares), and sample 3 (triangles).

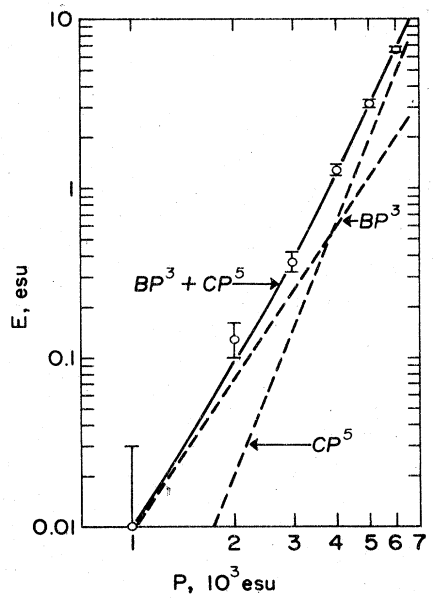

FIG. 8. Comparison of experimental points for determining critical exponent δ for KH_2PO_4 at 3 kbar, with theoretical expression (solid line) and its component terms (dashed lines) obtained from best fit to Landau theory.

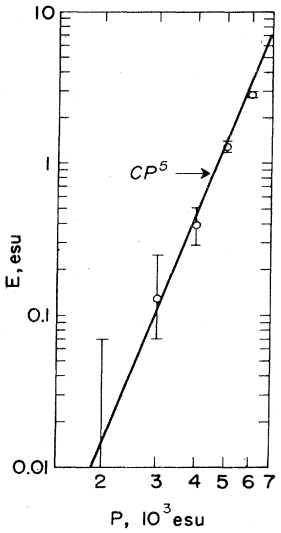

FIG. 9. Comparison of experimental points for determining critical exponent δ for KH_2PO_4 at 2.4 kbar, with theoretical expression CP^5 using C from Table X. Points represent fields for which $T = T_0$ for isopols in third run, Table IX.

also fall in the crossover region and show similarly good agreement with the field calculated from Eq. (12). In those plots, data points for the two branches corresponding to the "+" and "−" signs in Eq. (12) are clearly separated. Accordingly, these results for the critical exponent δ show the asymmetry of the wing critical points and the crossover from critical to tricritical behavior.

At 2 kbar we obtained[37] an effective value of 5.6 for δ, slightly larger than 5 as expected for the effective value for a first-order transition near the tricritical point. At 2.4 kbar we obtained for δ the three values 5.7 ± 0.5, 5.0 ± 0.8, and 4.5 ± 0.4 which correspond respectively to the first, second, and third run results shown in Table IX. The data points for δ obtained from the third run are shown in Fig. 9. The weighted average for the three runs is 4.9, with a standard deviation of 0.3 which seems optimistic because it does not overlap two of the three individual run values. The agreement of these values with the Landau-theory tricritical value of $\delta = 5$ is an additional indication that the tricritical point is near 2.4 kbar. These are the first measurements of the exponent δ near the tricritical point for any material.

Additional evidence for a tricritical point in KDP is provided by neutron diffraction measurements made by a group at Grenoble[40] of the temperature dependence of the change Δc of the unit cell length c at two pressures. Because Δc is proportional to the square of the spontaneous polarization P_s, they were able to determine the exponent β defined by $P_s \propto (T_{cr} - T)^{\beta}$. They found that β is near the Landau-theory tricritical value of $\frac{1}{4}$ at 2 kbar, and near the Landau-theory critical value of $\frac{1}{2}$ at 3.5 kbar.

VII. SUMMARY

We have measured the net polarization charge of two KH_2PO_4 crystals as a function of applied electric field in a 0.5-K neighborhood of the ferroelectric transition at hydrostatic pressures of 0, 1, 2, 2.4, and 3 kbar. In each case the paraelectric region is well described by the equation of state which follows from the Landau phenomenological expression for the free energy. The transition is first order at 0 and 1 kbar, with critical fields of 183 ± 60 V/cm at 0 kbar and 43 ± 13 V/cm at 1 kbar, and is second order at 3 kbar.

The pressure dependence of the coefficient B in the Landau equation of state $E = A_0(T - T_0)P + BP^3 + CP^5$ indicates a tricritical point (TCP) at 2.3 ± 0.3 kbar. Tricritical values predicted by Landau theory were observed by us for the exponents γ and δ and by Vettier, Bastie, and co-workers[40] for the exponent β. This TCP exists in the space of temperature, pressure, and electric field, hence the "wing" structure of the TCP is experimentally accessible.

ACKNOWLEDGMENTS

We thank J. R. Brookeman and T. A. Scott for the pressure-vessel design and for instruction in high-pressure lore. Experimental advice and assistance were supplied by R. J. Pollina in early stages of this work. Helpful discussions with K. Okada and E. K. Riedel are gratefully acknowledged. This work was supported by the NSF through Grant No. DMR 74-13220 A01. This work was based in part on a Ph.D. thesis submitted by A. B. Western and an M. S. thesis submitted by C. R. Bacon to Montana State University.

---

*Present address: Department of Physics and Geophysics, Montana College of Mineral Science and Technology, Butte, Montana 59701.
†Present address: EG&G, Idaho Falls, Idaho 83401.
‡Present address: Gray Tool Co., 7135 Ardmore, Houston, Texas 77002.

[1] R. B. Griffiths, Phys. Rev. Lett. 24, 715 (1970).

[2] A staggered field can be induced by an ordinary applied field for certain orientations of some compensated antiferromagnets, as shown by R. Alben, M. Blume, L. M. Corliss, and J. M. Hastings, Phys. Rev. B 11, 295 (1975). N. Giordano and W. P. Wolf, Phys. Rev. Lett. 39, 342 (1977) have employed such an induced staggered field to investigate the full three-dimensional phase diagram near the tricritical point in dysprosium aluminum garnet.

[3]*Collected Papers of L. D. Landau,* edited by D. ter Haar (Gordon and Breach, New York, 1965), pp. 193–216.
[4]V. H. Schmidt, Bull. Am. Phys. Soc. 19, 649 (1974).
[5]P. S. Peercy, Phys. Rev. Lett. 35, 1581 (1975).
[6]The earliest report of a first-order property of which we are aware is by P. P. Craig, Phys. Lett. 20, 140 (1966). Careful measurements by Reese (Ref. 13) in 1969 established the first-order nature of the transition.
[7]B. A. Strukov, M. A. Korzhuev, A. Baddur, and V. A. Koptsik, Fiz. Tverd. Tela (Leningrad) 13, 1872 (1971) [Sov. Phys. Solid State 13, 1569 (1972)].
[8]E. V. Sidnenko and V. V. Gladkii, Kristallografiya 18, 138 (1973) [Sov. Phys. Crystallogr. 18, 83 (1973)].
[9]M. Vallade, Phys. Rev. B 12, 3755 (1975).
[10]H. Sugié, K. Okada, and K. Kan'no, J. Phys. Soc. Jpn. 33, 1727 (1972).
[11]K. Okada, H. Sugié, and K. Kan'no, Phys. Lett. 44A, 59 (1973).
[12]K. Okada and H. Sugié, Ferroelectrics 17, 325 (1977).
[13]W. Reese and L. F. May, Phys. Rev. 162, 510 (1967); W. Reese, *ibid.* 181, 905 (1969).
[14]J. W. Benepe and W. Reese, Phys. Rev. B 3, 3032 (1971).
[15]J. Kobayashi, Y. Uesu, and Y. Enomoto, Phys. Status Solidi B 45, 293 (1971).
[16]T. Matsuda and R. Abe, J. Phys. Soc. Jpn. 36, 765 (1973).
[17]J. Eberhard and P. Horn, Solid State Commun. 16, 1343 (1975).
[18]A. B. Western and V. H. Schmidt, Solid State Commun. 19, 885 (1976).
[19]A. B. Western, A. G. Baker, R. J. Pollina, and V. H. Schmidt, Ferroelectrics 17, 333 (1977).
[20]V. H. Schmidt, A. B. Western, and A. G. Baker, Phys. Rev. Lett. 37, 839 (1976).
[21]R. T. Birge, Rev. Mod. Phys. 19, 298 (1947).
[22]H. Umebayashi, B. C. Frazer, G. Shirane, and W. B. Daniels, Solid State Commun. 5, 591 (1967).
[23]E. Hegenbarth and S. Ullwer, Cryogenics 7, 306 (1967).
[24]G. Samara, Phys. Rev. Lett. 27, 103 (1971).
[25]Cleveland Crystals, Inc., Box 3157, Cleveland, Ohio, 44117.
[26]Lake Shore Cryotronics, Inc., 9631 Sandrock Road, Eden, N. Y. 14057.
[27]Flexible Silver Coating No. 16, Hanovia Liquid Gold Division, Englehard Industries, Inc., East Newark, N. J. 07102.
[28]P. Bornarel, A. Fousková, P. Guyon, and J. Lajzerowicz, *Proceedings of the International Meeting on Ferroelectricity* (Inst. Phys. Czech. Acad. Sci., Prague, 1966), Vol. II, p. 81.
[29]Berylco-25, Kawecki Berylco Industries, Inc., 220 E. 42nd St., New York, N. Y. 10017.
[30]Model CSC 400 Cryogenic Capacitance Controller, Lake Shore Cryotronics, Inc. (see Ref. 26).
[31]W. N. Lawless, Rev. Sci. Instrum. 42, 561 (1971); *ibid.* 46, 625 (1975).
[32]F. A. Laws, *Electrical Measurements* (McGraw-Hill, New York, 1917), Chap. IV, pp. 175–177.
[33]Before measurements on sample 3 were begun, P. S. Peercy of Sandia Laboratories kindly repaired this leak by forcing Isopar *H* hydraulic fluid into the cone seal of the manganin cell at a pressure of 10 kbar.
[34]CARY 401 Vibrating Reed Electrometer, Cary Instruments, 2724 South Peck Road, Monrovia, Calif. 91016.
[35]A. B. Western, Jr., Ph.D. thesis (Montana State University, Bozeman) (unpublished), available through Xerox Microfilms, Ann Arbor, Mich. 48105.
[36]C. R. Bacon, M.S. thesis (Montana State University, Bozeman) (unpublished).
[37]Preliminary values for sample 3 at 2 kbar were reported by A. G. Baker, C. R. Bacon, and V. H. Schmidt, Bull. Am. Phys. Soc. 22, 324 (1977).
[38]S. Torstveit (private communication).
[39]A description of this criterion appears in J. M. Kincaid and E. G. D. Cohen, Phys. Rep. C 22, 57 (1975). These authors also illustrate additional phenomena which can occur if the P^8 term is retained.
[40]C. Vettier, P. Bastie, and M. Vallade, in High Pressure and Low Temperature Physics (Plenum, New York, to be published); P. Bastie, M. Vallade, C. Vettier, and C. M. E. Zeyen, Ferroelectrics (to be published); P. Bastie, M. Vallade, C. Vettier, and C. M. E. Zeyen, Phys. Rev. Lett. 40, 337 (1978).